International Journal of Statistics and Applied Mathematics 2022; 7(3): 37-42

International Journal of Statistics and Applied Mathematics

ISSN: 2456-1452
Maths 2022; 7(3): 37-42

www.mathsjournal.com
Received: 23-03-2022
Accepted: 25-04-2022

HZ Mawa
Department of Civil Engineering, Presidency University, Dhaka-1212, Bangladesh

Md. Yusuf Ali
Department of Civil Engineering, Presidency University, Dhaka-1212, Bangladesh

Jahedul Islam
Department of Civil Engineering, Presidency University, Dhaka-1212, Bangladesh

Corresponding Author:
HZ Mawa
Department of Civil Engineering, Presidency University, Dhaka-1212, Bangladesh

Mixed convection heat transfer effects in a lid driven square cavity

HZ Mawa, Md. Yusuf Ali and Jahedul Islam

DOI: https://doi.org/10.22271/maths.2022.v7.i3a.822

Abstract
This investigation numerically explored the parameters of mixed convection heat transfer in a square cavity with a bottom heated wall. The upper horizontal wall of the cavity is Tc, while the heated lower wall is T_h, while the surfaces of the left and right walls are adiabatic. The main approach here is to solve numerically the mass, momentum, and energy flow equation using Galerkin weighted residual finite element method. Here, the Prandtl number (Pr), Richardson number (Ri), and Reynolds number (Re) effects have been investigated. The factors mentioned above have been found to have a significant impact on the temperature and flow fields.

Keywords: Lid-driven cavity, mixed-convection, finite element scheme

Introduction

A shared forced and free convection flow of conductive fluid in a cavity in the presence of a fluid flow field has outstanding technological importance due to its multiple instances in many industrial applications, such as thermal insulation, geothermal reservoirs, and oil reservoirs. These problems can also arise while using microelectronic devices and electronic packaging. Mixed convective heat transfer through a lid-driven cavity has attracted much attention due to its importance in many technological forms, including solar collector design, crystal growth, thermal design of buildings, nuclear reactors, air conditioning, and more recently, solar energy, and collector design. The two warning regimes should often be considered when studying mixed convective flow [1, 2, 3]. Mixed convection heat transfer in a cavity determined by the lid was investigated by Prasad and Koseff 1996 [4]. They performed a series of experiments in a water-filled cavity and measured the heat flux at unusual locations on the hot floor of the cavity for a range of Re and Gr. Their review represents that the total heat transfer rate (i.e., area-averaged) is a weak function of Gr. Rahman *et al*. 2009 [5] considered the complexity of mixed convection flow within a ventilated rectangular cavity with a centered heat-conducting four-sided figure cylinder. The fluid flow characteristic of combined convection in a lid-driven cavity with a circular body where the left wall of the cavity was heated has been analyzed by Oztop *et al*. 2009 [6]. Saeidi and Khodadadi 2006 [7] presented a constant laminar forced convection flow problem in a square cavity with inlet and outlet ports. Very recently, Prakash and Ravikumar 2013 [8] investigated the thermal calm in a room with windows in the nearby walls together with other complementary elements. Using a velocity-vorticity concept, Senthil Kumar *et al*. 2009 [12] investigated double diffusion mixed convection in a square cavity by a lid-driven. Non-stationary mixed laminar convective heat transfer in a two-dimensional square cavity was investigated numerically by Aminossadati and Ghasemi 2008 [10]. Vishnuvard hanaraoi and Das 2008 [11] investigated laminar mixed convection in a parallel square chamber with a two-sided lid and differential heating filled with a liquid-saturated porous medium. Kumar *et al*. 2009 [12] used the multiple lattice approach to investigate mixed convection in a four-sided cavity with a porous medium. Chamkha *et al*. 2011 [13] numerically investigated the two-dimensional mixed convection of a heat source.

Consistent with the previous literature review, there has been little significant work on time-dependent mixed convection in a lid-driven square cavity with a heat-generating body. In the current study, thermal flow fields are observed due to the effects of Pr and Re.

Physical Configuration and Mathematical Formulation

We measured a two-dimensional (2-D) square enclosure of length L filled with an incompressible fluid with boundary conditions (Fig.1). From the demonstration sight, the upper wall is cold at temperature T_c and the bottom wall is heated which is kept at heat T_h, maintaining $T_h > T_c$. The other parts of the two vertical walls are adiabatic and the right vertical wall is a sliding wall.

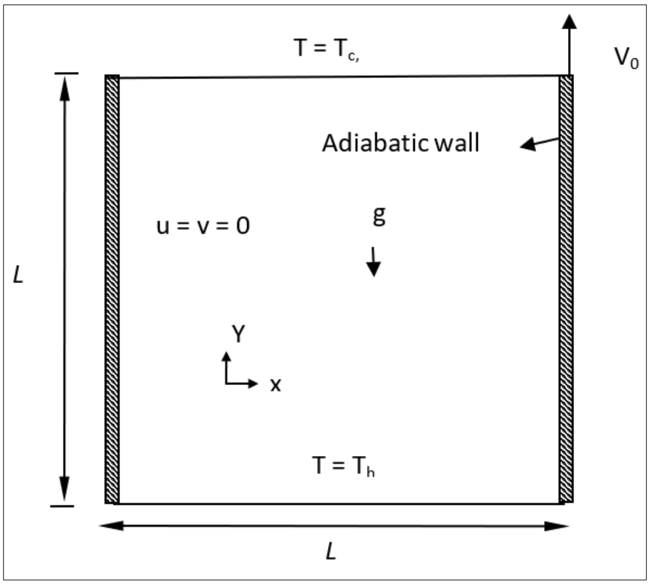

Fig 1: Schematic of the problem with the domain and boundary conditions

According to said assumptions, the governing equations for unsteady 2-D mixed convection flow in an enclosure using conservation of mass, momentum, and energy equation can be written with the following dimensionless forms:

$$\frac{\partial U}{\partial X} + \frac{\partial V}{\partial Y} = 0 \tag{1}$$

$$\frac{\partial U}{\partial t} + U\frac{\partial U}{\partial X} + V\frac{\partial U}{\partial Y} = -\frac{\partial P}{\partial X} + \frac{1}{\mathrm{Re}}\left(\frac{\partial^2 U}{\partial X^2} + \frac{\partial^2 U}{\partial Y^2}\right) \tag{2}$$

$$\frac{\partial V}{\partial t} + U\frac{\partial V}{\partial X} + V\frac{\partial V}{\partial Y} = -\frac{\partial P}{\partial X} + \frac{1}{\mathrm{Re}}\left(\frac{\partial^2 V}{\partial X^2} + \frac{\partial^2 V}{\partial Y^2}\right) + Ri\theta \tag{3}$$

$$\frac{\partial \theta}{\partial t} + U\frac{\partial \theta}{\partial X} + V\frac{\partial \theta}{\partial Y} = \frac{1}{\mathrm{Re\,Pr}}\left(\frac{\partial^2 \theta}{\partial X^2} + \frac{\partial^2 \theta}{\partial Y^2}\right) \tag{4}$$

where, the converted initial and boundary circumstances are:

t = 0, Entier Domain: $U = V = 0,\ \theta = 0,$

t > 0, at top wall $U = 0,\ V = 0,\ \theta = 0$

At left and right wall:

$$U = 0,\ V = 0,\ \frac{\partial \theta}{\partial N} = 0 \quad and \quad U = 0,\ V = 1,\ \frac{\partial \theta}{\partial N} = 0\ .$$

At the bottom wall: $U = V = 0, \theta = 1$ (on the heater)

where N is the dimensionless distance (either along the X or Y direction acting normal to the surface). (The governing equations, initial and boundary conditions are transformed into dimensionless forms using the following dimensionless variables:

$$U = \frac{u}{V_o},\ V = \frac{v}{V_o},\ P = \frac{p}{\rho\, {V_0}^2},\ \theta = \frac{(T - T_c)}{(T_h - T_c)},$$

As listed in the nomenclature, all variables have their normal sense in fluid mechanics and heat transfer. It can be seen from the above Eqs. (2)–(4), five parameters that preside over this problem are the Reynolds number (Re), Prandtl number (Pr), and Richardson number (Ri) which are defined respectively as

$$Re = \frac{V_o L}{v},\ Pr = \frac{v}{\alpha}, Ri = \frac{Gr}{\mathrm{Re}^2} = \frac{\alpha g \beta \Delta T L}{{V_0}^2},$$

where $\Delta T = T_h - T_c$ are the temperature difference of fluid respectively. The average Nusselt number at the heated wall may be expressed as

$$Nu_{av} = -\int_0^1 \frac{\partial \theta}{\partial Y}\, dX$$

The non-dimensional stream function is defined as:

$$U = \frac{\partial \psi}{\partial y}, V = -\frac{\partial \psi}{\partial x}).$$

Numerical Implementation

The Galerkin weighted residual finite element method is used to convert the nonlinear governing partial differential equations, such as mass, momentum, energy, and concentration equations, into a system of integral equations. Zienkiewicz and Taylor 1991 [15] discuss the procedure in detail. The Gauss quadrature method is used to achieve the integration in each term of these equations. With the use of boundary conditions, Newton's technique is used to convert non-linear algebraic equations into linear equations. Finally, we solve these linear equations using the triangular Factorization technique. The convergence of solutions is assumed when the relative error for each variable between consecutive iterations is recorded below the convergence criterion ε such that $|\Gamma m + 1 - \Gamma m| \le 10^{-4}$, where m is the number of iterations and Γ is the general dependent variable

Grid sensitivity check

Initially, la grid sensitivity check is conducted to choose the proper grid for the numerical prediction. Five different types of the grid are considered for the grid refinement analysis: 3776, elements, 4934, elements 5148, elements; 6326 elements, and 8506 elements. The deviations among the results are very few as shown in Table-1. Therefore, the grid results with 5148 elements are selected throughout the simulation.

Table 1: Grid sensitivity check at Re = 100, Ri = 1 and Pr = 0.71

No. of elements	3776	4934	5148	6326	8506
Ave. Nu	4.633661	4.617892	4.646701	4.649664	4.653317

Code Validation

The computational results are compared with the literature Ching [16] for validation of the present numerical code. The physical problem studied by Ching [16] was a lid-driven triangular enclosure. The length and height of the enclosures are depicted by L respectively. The calculated average Nusselt numbers are shown in Table 2. It can be seen from the figures that the present results and those reported in Ching [16] are in excellent agreement. This validation boosts the confidence in the numerical outcome of the present work.

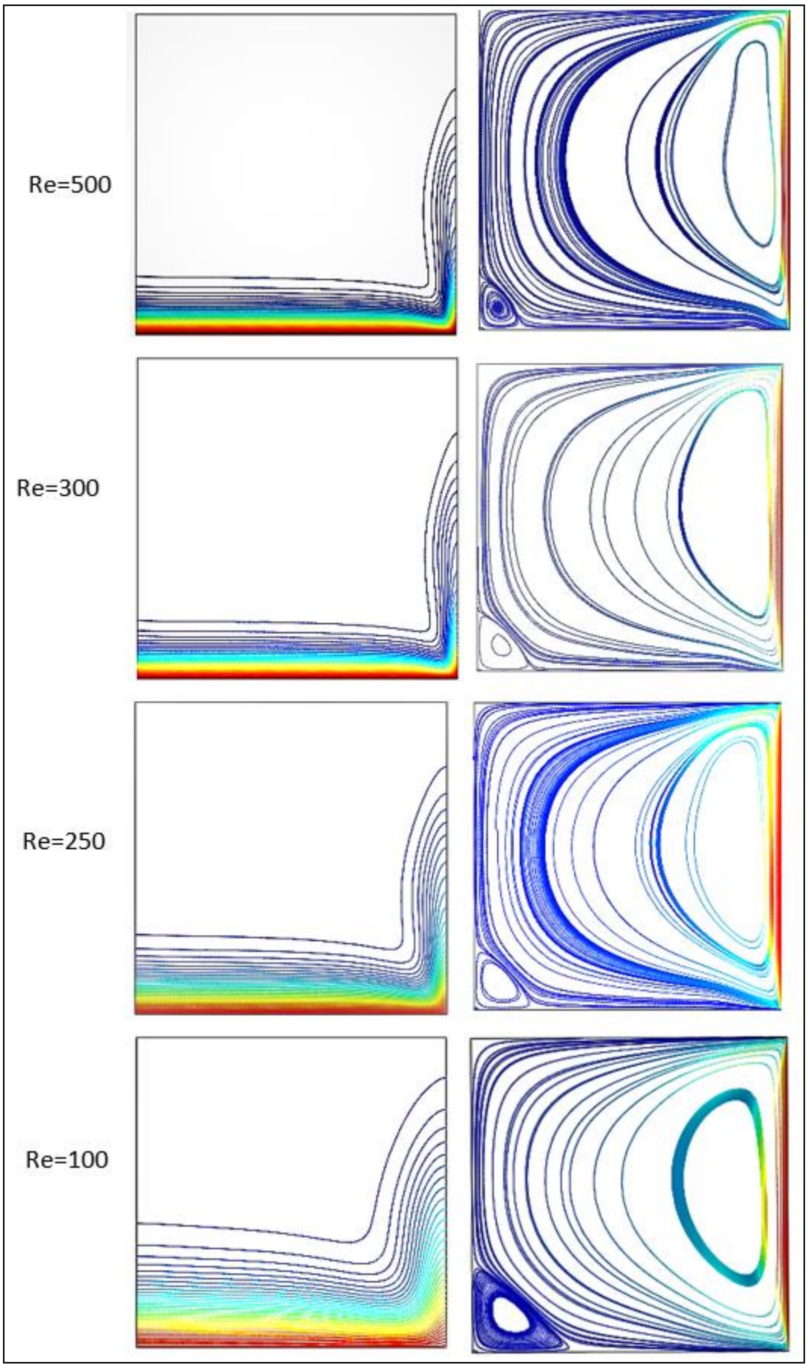

Fig 2(a) Fig 2(b)

Fig 2: Effect of Reynolds number (*Re*) on (a) isotherms and (b) streamlines for the selected values of $Ri = 1$, $Pr = 0.71$,

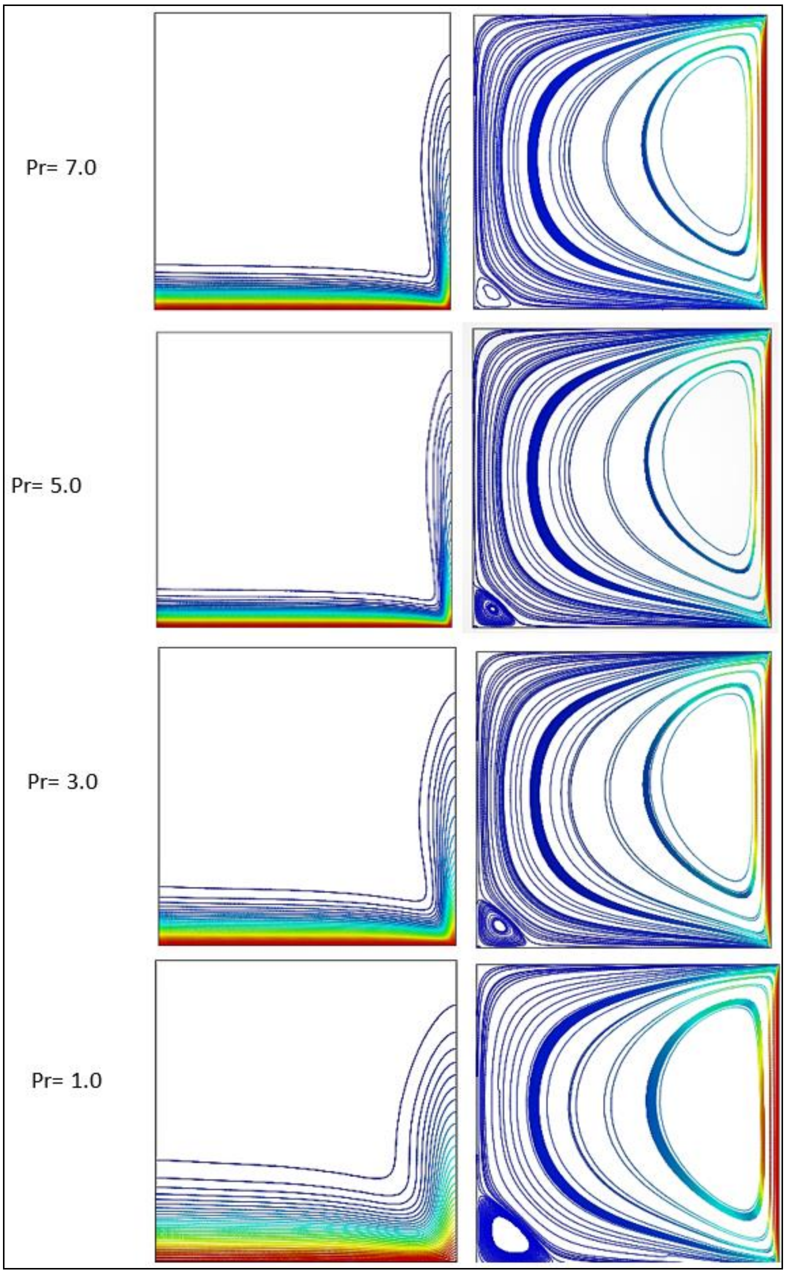

Fig 3(a) Fig 3 (b)

Fig 3: Effect of Prandle number (*Pr*) on (a) isotherms and (b) streamlines for the selected values of *Re* = 100, *Ri* = 1.

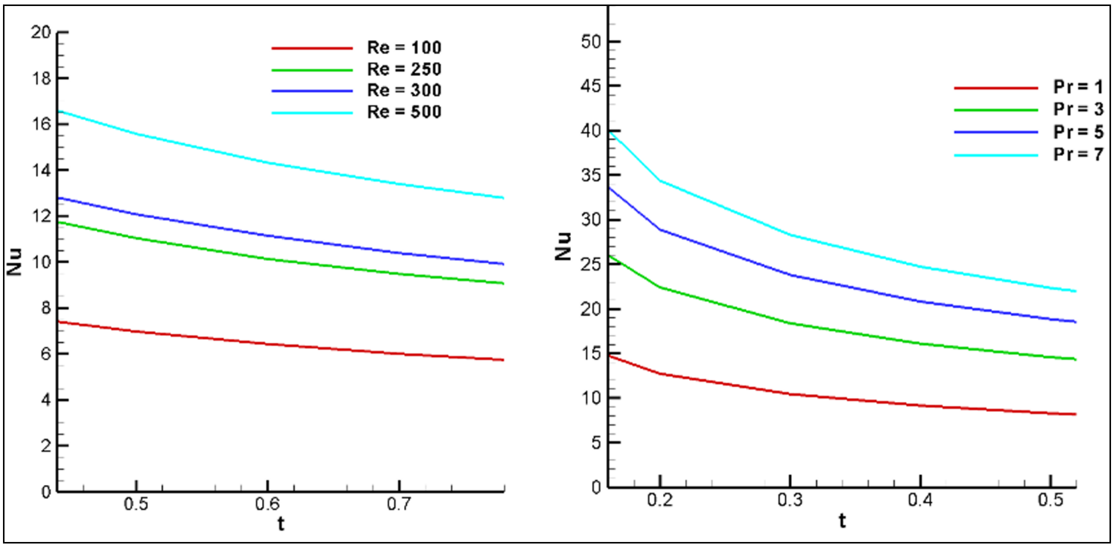

Fig 4(a) Fig. 4(b)

Fig 4: Effects of average Nusselt number for (a) Reynolds number (b) Prandtl number,

Table 2: Comparison of average Nusselt number between the present numerical solution and that of Ching [16] at Pr= 0.71, Re= 100, Ri =1

Ri	Present	Ching [16]
0.1	27.991	28.653
1	11.152	12.231
10	11.027	11.569

Results and Discussions

The numerical final results have been offered that installation the effects of the presence of dimensionless parameters in a cavity. The dimensionless governing parameters that have to be designated for the device are Reynolds number (Re), and Prandtl number (Pr). Since such a lot of primary dimensionless parameters are required to characterize a system, a complete evaluation of all combinations of those parameters isn't practical. The numerical outcomes have been used to explain the impact of numerous parameters at a small fraction of the possible conditions via way of means of simplifying the configuration. The shows of the outcomes had been commenced with the streamline and isotherm patterns in the cavity. Demonstrative distributions of the average Nusselt number on the heated wall with inside the cavity have additionally been provided.

Effect of Reynolds number

The effects of the isotherm line and streamlines for various Re values are shown in fig. 2. The number Re here ranges from 100 to 500. At first, the isotherms line may be visible in both the heating and right-side walls. In fig 2(a), isotherms lines at lower walls become significantly concentrated as this value grows. Fig. 2(b) shows the relevant velocity distributions. The consequences of streamlining for various values of Re are depicted in fig.2 (b). More streamlines are evident because of the high Reynolds number, but streamlines are less prominent at Re =100 and Re =250 compared to Re=500. At first, a tiny vortex can be visible in the enclosure's left bottom corner, but it gets smaller as Re=500 approaches. Moreover when Re increases up to the value of 500, the part: forced convection in the cavity becomes more significant, and consequently, the circulation in the flow becomes large with clear inner vortices as presented in fig. 2(b). The average Nusselt numbers at the heat source in the cavity have been plotted for particular Reynolds numbers that are shown in fig. 4(a) average heart rate for all values is temperately increased, however after some time they are decreasing naturally.

Effect of Prandtl number

Fig. 3(a) and 3(b) display the impact of Pr on isotherms and streamlines, respectively. The isotherms lines almost parallel to the heated partitions at very low Pr (=1.0), simulating a conduction-like heat switch in the cavity, at the same time as the decreased heated wall isotherms are almost wavy in fig. 3(a). As Pr rises, the depth of the thermal boundary layer in the site close to the temperature-producing site increases. Isothermal lines additionally vanish from the higher location of the wall. Figure 3(b) demonstrates the effect of the streamline for diverse Pr values. For the aforementioned values of Pr, fluid rises alongside the place of the vertical partitions, forming a roll with clockwise rotating cells which are the same in look besides for close to the heated clean wall. The flow field remains nearly regular despite the variation in Pr. The common heat transfer rate for different values of Pr is discovered in fig. 4(b), however, after a few times, those values drop slightly.

Conclusion

The outcomes of the Re and Pr numbers on mixed convective flows with the thermal field have been explored in this work. According to the findings, better Reynolds numbers bring about a considerable increase in heat transmission from the heated wall. In a place ruled with the aid of using pressured convection, Prandtl variety outcomes in flow behaviors are greater substantial. With growing Reynolds and Prandtl numbers, the heat switch at the bottom heated surface increases.

Nomenclature

Re	Reynolds number
Pr	Prandtl number
Gr	Grashof number
Ri	Richardson number
L	length of the enclosure
Nu_{av}	Average Nusselt number
T	dimensionless temperature
P	non-dimensional pressure
X, Y	dimensionless coordinates
U, V	dimensionless velocity components
C	concentration
ΔT	Temperature difference
ΔC	Concentration difference
Greek symbols	
μ	dynamic viscosity
ν	kinematic viscosity
α	thermal diffusivity
h	convective heat transfer coefficient
ρ	density
Ψ	stream function
Subscripts	
av	Average
h	Hot
c	Cold

References

1. Schriber R, Keller HB. Driven cavity flows by efficient numerical techniques. J Comput. Phys. 1983 Feb 1;49(2):310-33.
2. Ideriah FJK. Prediction of turbulent cavity flow driven by buoyancy and shear. J Mech. Engng. Sci. 1980 Dec;22(6):287-95.
3. Moallemi MK, Jang KS. Prandtl number effects on laminar mixed convection heat transfer in a lid-driven cavity. Int. J Heat Mass Transfer. 1992 Aug 1;35(8):1881-92.
4. Prasad AK, Koseff JR. Combined forced and Natural convection heat transfer in a deep lid-driven cavity flow. Int. J Heat Fluid Flow. 1996 Oct 1;17(5):460-7.
5. Rahman MM, Elias M, Alim MA. Mixed convection flow in a rectangular ventilated cavity with a heat-conducting square cylinder at the center. J of Engineering and Applied Sciences. 2009;4(5):20-29.
6. Oztop HF, Zhao Z, Yu B. Fluid flow due to combined convection in a lid-driven enclosure having a circular body. Int. J. Heat and Fluid Flow. 2009 Oct 1;30(5):886-901.
7. Saeidi SM, Khodadadi JM. Forced convection in a square cavity with inlet and outlet ports. Int. J of Heat and Mass Transfer. 2006 Jun 1;49(11-12):1896-906.
8. Prakash D, Ravikumar P. Study of thermal comfort in a room with windows at adjacent walls along with additional vents. Indian J of Sci. and Tech. 2013;6(6):4659-4669.

9. Senthil Kumar D, Murugesan K, Thomas HR. Numerical Simulation of Double Diffusive Mixed Convection in a Lid-Driven Square Cavity using Velocity-Vorticity Formulation, Numer. Heat Transfer A. 2008;54(9):837-865.
10. Aminossadati SM, Ghasemi B. Comparison of Mixed Convection in a Square Cavity with an Oscillating Versus a Constant Velocity wall, Numer. Heat Transfer A. 2008;54(7):726-743.
11. Vishnuvard hanarao E, Dass MK. Laminar Mixed Convection in a Parallel Two-Sided Lid-Driven Differentially Heated Square Cavity Filled with a Fluid-Saturated Porous Medium, Numer. Heat Transfer. 2008;53(1):88-110.
12. Kumar DS, Dass AK, Dewan A. Analysis of Non-Darcy Models for Mixed Convection in a Porous Cavity using a Multigrid Approach, Numer. Heat Transfer. 2009;56(8):685-708.
13. Chamkha AJ, Hussain SH, Abd-Amer QR. Mixed Convection Heat Transfer of Air Inside a Square Vented Cavity with a Heated Horizontal Square Cylinder, Numer. Heat Transfer. 2011;59(1):58-79.
14. Shi W, Vafai K. Mixed Convection in an Obstructed Open-Ended Cavity, Numer. Heat Transfer. 2010;57(10):709-729.
15. Zienkiewicz OC, Taylor RL. The finite element method, Fourth Ed., McGraw-Hill; 1991.
16. Ching YC, Öztop HF, Rahman MM, Islam MR. Ahsan, A. Finite element simulation of mixed convection heat and mass transfer in a right triangular enclosure. Int. J Heat Mass Transf. 2012 May 1;39(5):689-96..